

# Failure Modes and Bearing Capacity Estimation for Strip Foundations in C- $\phi$ Soils: A Numerical Study

Paul Akagwu, Aaron Aboshio

**Abstract**—In this study, typical c- $\phi$  soils subjected to loadings were assessed with a view to understand the general stress distribution and settlement behaviour of the soils under drained conditions. Numerical estimations of the non-dimensional bearing capacity factors,  $N_q$  and  $N_c$ , for varied angles of friction in the soil mass were obtained using PLAXIS. Ultimate bearing capacity values over a  $\Phi$  range of 0-30 degrees were also computed and compared with analytical results obtained from the traditional simplified uncoupled approach of Terzaghi and Meyerhof. Results from the numerical study agree well with theoretical findings.

**Keywords**—Bearing capacity factors, finite element method, safe bearing pressure, structure-soil interaction.

## I. INTRODUCTION

FOUNDATION stability is largely a function of the mechanical behaviour of the soil on which it is laid. Varied soil types respond differently to imposed structural loads; hence, factors such as the soil texture, micro structural particles, cohesion and shear strengths, specific gravity, etc. are studied to understand behaviour under loads [1].

Over the years, several analytical and empirical models have evolved in soil mechanics to describe soil behaviour and more recently, numerical methods have become commonplace, one such being the Finite Element Method which is now widely used because of its inherent versatility.

At the sub-structural design phase, both structural and geotechnical analyses are essential to ensure adequate resistance to foundation rupture and/or compression to such a magnitude that the integrity of the superstructure is not compromised. Some important geotechnical factors that influence the foundation design include thickness of the bearing strata, compressibility and shrink-swell potential of the bearing strata, seasonal volume change, cut/fill requirement etc. [1] and ultimately the bearing capacity of the soil.

The general bearing capacity equation for c- $\phi$  soils can be written as:

$$q_{ult} = cN_c s_c d_c i_c + q_0 N_q s_q d_q i_q + \frac{1}{2} \gamma B N_\gamma s_\gamma d_\gamma i_\gamma \quad (1)$$

where  $s_c s_q s_\gamma$  = shape factors;  $d_c d_q d_\gamma$  = depth factors;  $i_c i_q i_\gamma$  = load inclination factors; and  $N_c$  = non-dimensional bearing capacity factors relating the influence of soil cohesion on bearing capacity;  $N_q$  = non-dimensional bearing capacity factors relating the influence of soil overburden on bearing capacity;  $N_\gamma$  = non-dimensional bearing capacity factors relating the influence of soil unit weight on bearing capacity.

Different equations have been suggested by a number of researchers for the estimation of these bearing capacity factors. The most common are those by Hensen [2], Vesic [3], Terzaghi [4] and Meyerhof [5].

Often, the ultimate bearing pressure is computed in an uncoupled manner, i.e. considering the strength contributions from the soil cohesion, effect of surcharge and unit weight of the soil separately and aggregating the three terms. This is largely considered a simplified approach to solving the complex equation presented in (1).

This study seeks to numerically assess the stress distribution and settlement behaviour of a typical c- $\phi$  soil as well as compute bearing pressures for the soils using both the simplified approach and the complex monolithic approach in order to compare results from the two methods. Secondly, bearing capacity factors and failure modes under loads of varied soil types are also computed.

## II. NUMERICAL MODEL

Due to both geometric and loading symmetry in a typical strip foundation, only a quarter of the structure was considered in this study while employing accordingly, symmetry boundary conditions in line with standard practice. This approach enhances meshing efficiency and reduces computation time without loss of accuracy. The strip foundation models are of unit width ( $B = 1$ ) and semi-infinite length consistent with other studies [6].

A depth-to-width ratio of 5 ( $H/B=5$ ) was used following preliminary studies to establish an optimum  $H/B$  ratio for the model so as to avoid interference of the soil boundaries with the soil deformation under loads. Manoharan et al. [6] adopted a ratio of 10 for a similar problem but for this case, a ratio of 5 which translates to reduced mesh number and computation time was found to be just as efficient in capturing the stress and deformation fields within the soil.

Paul Akagwu is a Subsea Engineer with Technip UK limited Aberdeen, United Kingdom (e-mail: pakagwu@gmail.com).

Dr. Aaron Aboshio is a Civil/Structural Engineering Lecturer at Bayero University, Kano-Nigeria, PMB 3011 (e-mail: aaboshio.civ@buk.edu.ng).

III. FINITE ELEMENT DISCRETIZATION AND MESH REFINEMENT

The finite element discretization and analyses of the structure-soil-interaction problems were carried out using the PLAXIS code. For the problem, a plain strain model with 15 noded-triangular elements (Fig. 1) was used. This is to take advantage of the traditional characteristics of these elements; i.e. the ease of efficient element arrangement and refinement of the mesh at the vicinity of corners of the footings which is crucial for an accurate prediction of the collapse loads [7] as well as stresses at the footing-soil interface.

Fig. 1 also shows the model discretization, loading and boundary conditions adopted in this study.

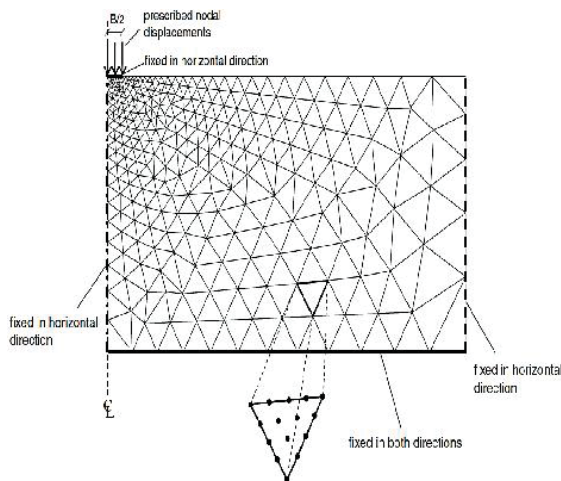


Fig. 1 Typical mesh and boundary condition used for the foundation-soil interaction simulations [8]

IV. SOIL MATERIAL PARAMETERS

The initial  $c-\phi$  soil model parameters considered in this study are presented in Table I.

TABLE I  
C- $\phi$  SOIL PARAMETERS

Symbol	Quantity	
$E'$	Elastic Modulus	5 MN/m <sup>2</sup>
$C'$	Cohesion	5 kN/m <sup>2</sup>
$\Phi'$	Angle of internal friction	22°
$\Psi$	Dilatancy Angle	0
$\nu'$	Poisson ratio	0.45
$\gamma$	Unit weight of soil	17 kN/m <sup>3</sup>
$q_0$	Surcharge	5 kN/m <sup>2</sup>

V. RESULTS AND DISCUSSIONS

A. Load-Settlement Behaviour

Fig. 2 shows results of the load-settlement profile of the  $c-\phi$  soil considered in this study. The results obtained from the numerical study are consistent with established theory on load-settlement curves for local shear failure in moderately compressible soils postulated by Vesic (Fig. 3) as reported by [9].

The shape of the curve implies that  $c-\phi$  soils at drained state, under loadings, would normally undergo significant settlement before ultimate bearing pressure limit is reached whereas, in purely cohesive soils, limit loads can easily be deduced from the load – settlement curves, that cannot be said about frictional soils as implied by the curve profile in Fig. 2. Consequently, two failure loads are usually defined, the first occurring at the upper limit of the elastic portion, the reason being that, even while deforming elastically, large deformations tend to occur. The plastic failure load is defined at the plastic zone. The settlement recorded in the frictional soil is higher than that reported for cohesive soils [10], [11].

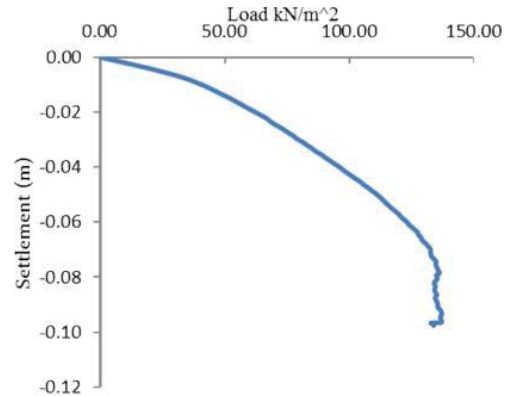


Fig. 2 Numerical Estimate of Load-Settlement Curve for  $c-\phi$  Soils

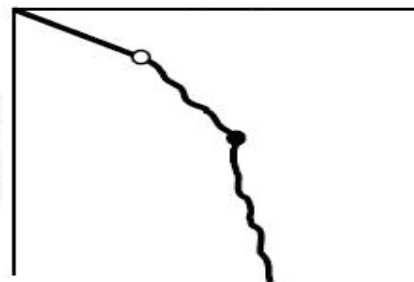


Fig. 3 Vesic's Load Settlement Curve for Local Shear Failure [9]

B. Stress Fields

1) Effective Stress Fields

Effective stress fields of the  $c-\phi$  soil under load are presented in Fig. 4 (a). This shows that the normal stress effect is higher under the foundation than anywhere within the soil mass. And within the foundation, the contact stress is higher at mid-point as shown in the longitudinal section plot of the stress field in Fig. 4 (b).

Stress-strain relation at the footing edge and mid-point are presented in Figs. 5 and 6. The result shows that the maximum stress at mid-point is about thrice that recorded at the edge of the footing.

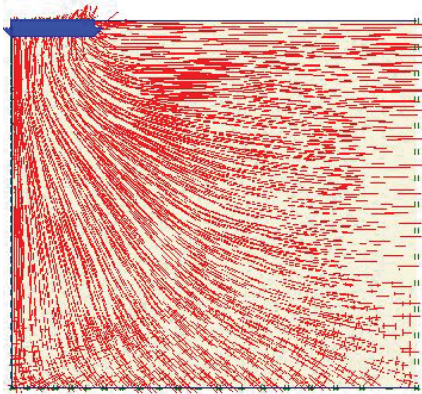


Fig. 4 (a) Effective Stress Field

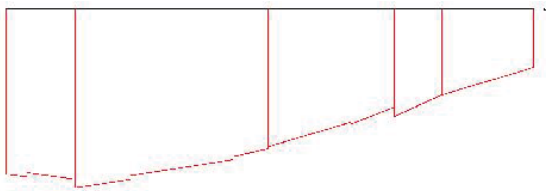


Fig. 4 (b) Longitudinal Section of the stress fields under the foundation

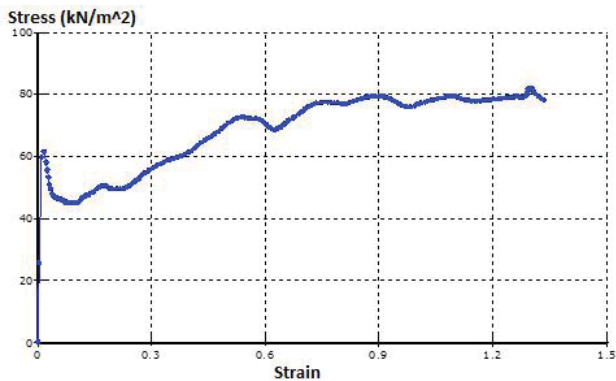


Fig. 5 Stress – Strain Curve at Edge of Footing

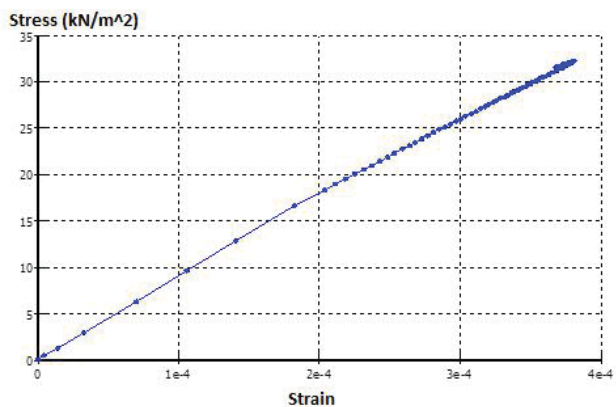


Fig. 6 Stress – Strain Curve at Midpoint of Footing

The total incremental displacements and strain contours are shown in Figs. 7 (a) and (b). These are typical of local shear failure mechanism in soils where due to the associated large settlements as presented in Fig. 2, failure occurs a little farther beneath the footing before the development of full Rankine zone.

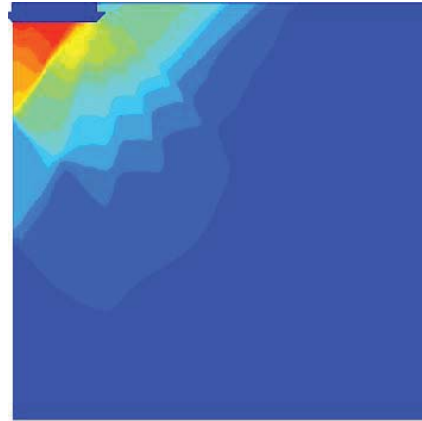


Fig. 7 (a) Total incremental displacement contours

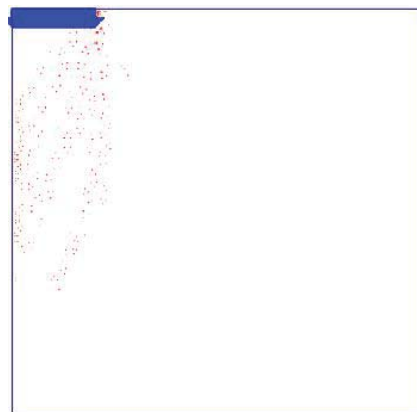


Fig. 7 (b) Total incremental strain contours

## VI. FAILURE PROPAGATION

Below are contour plots of the various stages of the propagation of plasticity within the soil model. At a load of about 50 kN/m<sup>2</sup> corresponding to the upper limit of the elastic zone in the load settlement curve of Fig. 2, slight plasticity begins to develop at the edge of the footing (Fig. 8 (a)). As the load increases, plasticity reaches the centerline of the footing (Fig. 8 (b)), and as the failure limit load is reached, a substantial portion of the model becomes plastic and failure happens with little heaving occurring at the footing sides (Fig. 8 (c)).

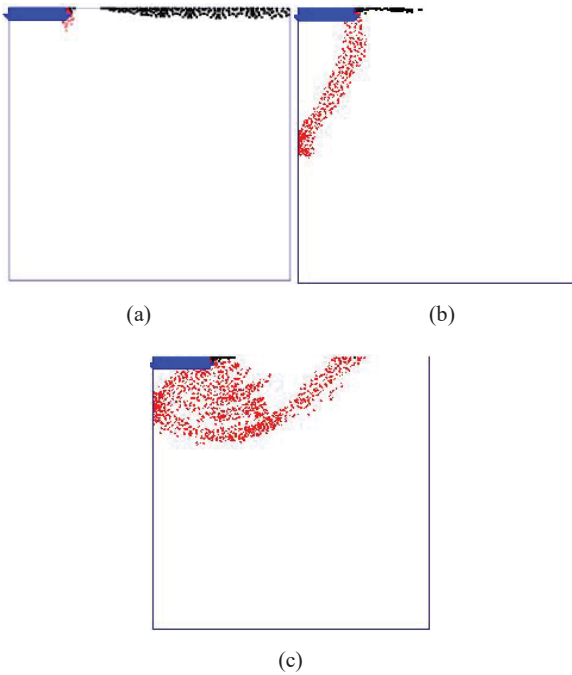


Fig. 8 Failure modes of frictional soils at the initial plastic state (a), Intermediate plastic state (b) and at ultimate failure state (c)

VII. DETERMINATION OF BEARING CAPACITY FACTORS  $N_\gamma$  AND  $N_q$  FOR SURFACE FOOTINGS

In this section, an attempt is made to generate bearing capacity factors,  $N_\gamma$  and  $N_q$  numerically, using PLAXIS, to enable a broad comparison with those found in the literature.

In determining  $N_\gamma$ , a unit soil weight ( $\gamma$ ) of 17 kN/m<sup>2</sup> was used, cohesion  $c$  was set to null and no surcharge load was applied to enable an independent assessment of the contribution of the soil wedge beneath the footing to the bearing capacity of the soil. Secondly,  $N_q$  was found by setting soil unit weight and cohesion to null and applying a surcharge load of 5kN/m<sup>2</sup> as shown in Fig. 9.

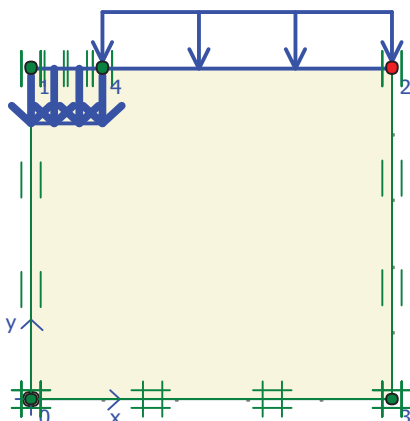


Fig. 9 Structural model showing surcharge loads for determining bearing capacity factors

A.  $N_\gamma$  Values

The results presented in Fig. 10 shows a close correlation between the analytical solutions for  $N_\gamma$  proposed by several Researchers and the numerical values obtained with PLAXIS. For internal friction ( $\Phi$ ) values between 0 and 30 degrees, the values of  $N_\gamma$  agree point to point with those of Meyerhof and Hansen. However, Vesic and Terzaghi's  $N_q$  values were found to be higher than the numerically generated values.  $N_\gamma$  was obtained by using the relation  $q = 0.5 B \gamma N_\gamma$ , such that  $N_\gamma = 2q / (B \gamma)$

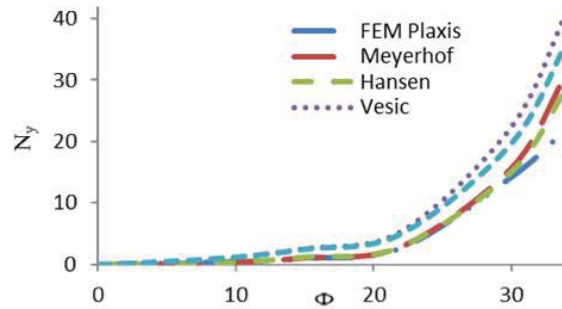


Fig. 10 Analytical and Numerical Values of  $N_\gamma$

B.  $N_q$  Values

Numerically generated values of  $N_q$  using PLAXIS are herein compared with those of Meyerhof [5], Hansen [2] and Terzaghi's [4] Fig. 11.  $N_q$  values are the same for the first three authors.  $N_q$  was obtained from the relation  $q = q_0 N_q$  such that  $N_q = q / (q_0)$ .

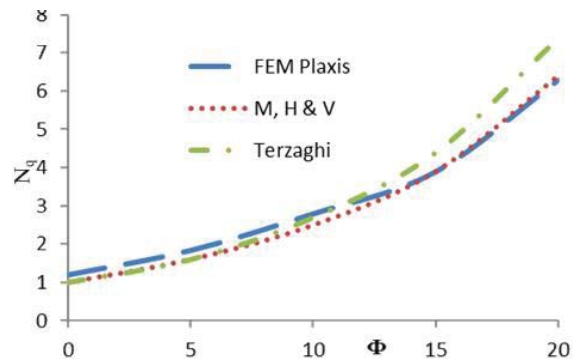


Fig. 11 Analytical and Numerical Values of  $N_q$

From Fig. 11, it is obvious that the numerical values for  $N_q$  fall closely within the range of the conventionally adopted analytical solutions.

VIII. COMPARISON OF BEARING CAPACITY VALUES OBTAINED BY COUPLED & UNCOUPLED ANALYSES

A. Analysis Using PLAXIS (Drained  $c - \phi$  Model)

Terzaghi's ultimate bearing capacity equation based on the theory of superposition is a convenient simplification of a complex analytical problem. Generating an analytical solution that incorporates the contributions from the three components of soil weight, cohesion and surcharge simultaneously is



cumbersome. However, with finite element analysis, the contributions of these components can be simultaneously measured. PLAXIS was used to obtain ultimate bearing capacity values over a  $\Phi$  range of 0-30 degrees and the results compared with those obtained using Terzaghi [4] and Meyerhof's [5] factors. Fig. 12 shows there is a close agreement between the values obtained from both modes of analysis. The PLAXIS curve tends to lie between those of Terzaghi [4] and Meyerhof [5] with their differences increasing with increasing  $\Phi$ . It suffices therefore to conclude that the superposition premise upon which ultimate bearing capacity formula is based is justified.

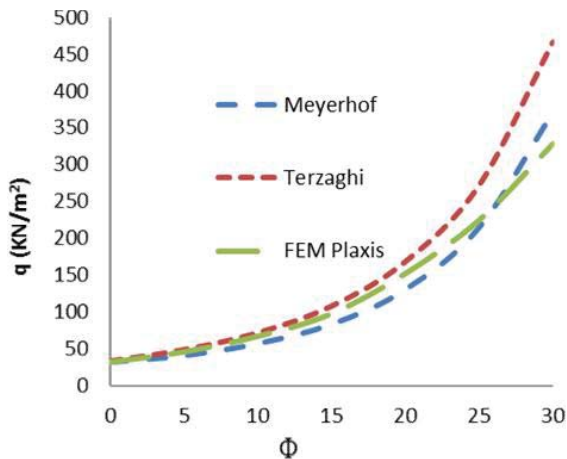


Fig. 12 Bearing Capacity Values for Superposition and Combined Analysis

#### IX. CONCLUSIONS

Numerical simulation of the response of frictional soils to structural loads as well as estimation of bearing capacities were carried out with PLAXIS and the specific findings from the study are as follows: C- $\phi$  soils at drained state, under loadings, undergo significant settlement before their ultimate bearing pressure limit is reached.

Numerically generated bearing capacity factors  $N_q$  and  $N_\gamma$  agreed reasonably with those of Terzaghi and other authors with negligible variations for  $\Phi$  range of 0-25 degrees. However, as  $\Phi$  approached 30 degrees, the difference in the analytical and numerical  $N$  - values increased steadily. Results show a realistic correlation between bearing capacity values obtained from combined analysis using PLAXIS and those analytically obtained based on superposition. Differences were in the neighbourhood of 0-12 %

The traditional simplified approach of considering the effect of each term of the bearing capacity equation separately and combining the three terms for the determination of bearing capacity is justified as there is a very negligible difference in results when compared with the complex approach of analyzing the whole terms as a single block.

#### REFERENCES

- [1] R. W. Stephensen, "Shallow foundations," in *Practical foundation engineering handbook*, Mc-Graw Hills Companies Ltd., 2004.
- [2] B. J. Hansen, "A revised and extended formula for bearing capacity," *Dan. Geotech. Inst. Bull.*, vol. 28, pp. 5–11, 1970.
- [3] A. S. Vesic, "Analysis of ultimate loads of shallow foundations," *J. Soil Mech. Found. Div. ASCE*, vol. 99, no. 1, pp. 45–73, 1973.
- [4] J. Bowles, *Foundation Analysis and Design*. Mc-Graw Hills Companies, 1997.
- [5] G. Meyerhof, "Some Recent Research on the Bearing Capacity of Foundations," *Can Geotech J*, vol. 1, pp. 16–26, 1963.
- [6] N. Manoharan et al: Bearing Capacity of Surface Footings by Finite Elements, *Computer & Structures* Vol. 54. No. 4, pp 563 – 586. (1995).
- [7] D. Pott and L. Zdravkovic, *Finite Element Analysis in Geotechnical Engineering: Theory*. London: Thomas Telford Ltd., 1999.
- [8] D. Loukidis and R. Salgado, "Bearing Capacity Of Strip And Circular Footings In Sand Using Finite Elements," *Comput. Geotech.*, Vol. 36, Pp. 871–879, 2009.
- [9] R. Day, *Foundation Engineering Handbook: Design and Construction with the 2006 International Building Code*. Mc-Graw Hills Companies Ltd., 2006.
- [10] A. Aboshio, "Static Response To Homogeneous Clay Stratum To Imposed Structural Loads," *Int. J. Environ. Chem. Ecol. Geol. Geophys. Eng.*, Vol. 9, No. 12, 2015.
- [11] P. Akagwu, "Finite Element Modelling of Strip Foundations with PLAXIS." MSc Foundation Engineering Coursework Report, University Of Leeds, UK, 2009.